

Spectroscopic Studies on Adsorbed Metal Carbonyls. Part 1. Interaction of $[\text{Rh}_4(\text{CO})_{12}]$ and $[\text{Rh}_6(\text{CO})_{16}]$ with Alumina, Silica, and Titania †

John Evans* and Gregory S. McNulty

Department of Chemistry, The University, Southampton SO9 5NH

The interaction of $[\text{Rh}_4(\text{CO})_{12}]$ (1) and $[\text{Rh}_6(\text{CO})_{16}]$ (2) with Al_2O_3 , TiO_2 , and SiO_2 has been monitored by i.r. spectroscopy, using isotopic substitution and spectrum simulation techniques. Conversion of (1) into (2) has been demonstrated on Al_2O_3 and TiO_2 . Isolated $\text{Rh}^1(\text{CO})_2$ sites are considered to exist on all three oxides after oxidative fragmentation of (1) or (2). $\text{Rh}(\text{CO})_n$ ($n = 3$, or possibly 4) sites were also suggested from (1) and TiO_2 or SiO_2 . Extended reaction times (TiO_2 and Al_2O_3) or exposure to the i.r. spectrometer beam (Al_2O_3) causes aggregation to metal crystallites.

Since the early investigation of new catalytic materials from the interaction of $[\text{Ru}_3(\text{CO})_{12}]$ with silica,¹ there has been considerable interest in the reactions between metal carbonyl clusters and oxides. Starting from a particular cluster nuclearity, interaction may maintain the original skeleton, aggregate, or fragment, perhaps oxidatively. We wish to specify some of these processes spectroscopically and in this paper we concentrate on the interaction of $[\text{Rh}_4(\text{CO})_{12}]$ (1) and $[\text{Rh}_6(\text{CO})_{16}]$ (2) with three Aerosil type oxides and extend the normal use of the intense carbonyl absorptions in the i.r. spectrum by use of mixed isotopes and spectral simulation to test various structural hypotheses. Isotopic mixing is generally a very effective method of establishing molecular shapes in high-resolution situations, but nevertheless it is valuable even with the degraded resolutions obtainable in the polar environment of an oxide surface. These particular cluster-oxide interactions have been studied previously²⁻¹⁰ and the oxidised carbonyl-bearing site of rhodium on alumina is among the best characterised, as a $\text{Rh}(\text{CO})_2$ unit¹¹ and can be used as a calibration for the techniques employed here. (This work can only yield structural information in detail about isolated carbonylated centres or those in close proximity.)

Experimental

Infrared and mass spectra were recorded on Perkin-Elmer 580B (with a model 3500 data station) and AEI MS12 instruments respectively. I.r. spectra were recorded as Nujol mulls.

$[\text{Rh}_4(\text{CO})_{12}]$ and $[\text{Rh}_6(\text{CO})_{16}]$ were prepared by the methods of Chini and Martinengo.¹² All hydrocarbon reaction solvents were stirred over H_2SO_4 to remove unsaturates, distilled off CaH_2 , and stored over molecular sieves. The oxides used were Aerosil 200 (SiO_2), Aluminoxid C (Al_2O_3), and Titanoxid P25 (TiO_2) from Degussa and were dried at 160°C *in vacuo* before use.

Preparation of ^{13}C -enriched $[\text{Rh}_4(\text{CO})_{12}]$.— $[\text{Rh}_4(\text{CO})_{12}]$ (0.1 g) was stirred in light petroleum (b.p. $40\text{--}60^\circ\text{C}$)– CH_2Cl_2 (30 cm^3) in a closed glass vessel (135 cm^3) under ^{13}C (220 Torr) for 15 h at room temperature. The ^{13}C enrichment level was determined as ca. 40% from matching isotopic distribution calculations to the observed mass spectrum. A similar value was obtained by measuring the intensity of the bridging $\nu(\text{CO})$ bands in the i.r. spectrum.

Solution Reactions of Rhodium Carbonyls with Oxides.— $[\text{Rh}_6(\text{CO})_{16}]$ or $[\text{Rh}_4(\text{CO})_{12}]$ (0.015 g) was dissolved in the appropriate hydrocarbon solvent (40 cm^3) and stirred with the oxide (0.2 g) for the required reaction time. The powder was filtered off from the reaction solution and dried *in vacuo*. Experiments in air and under a dry nitrogen atmosphere were carried out.

Interaction of Supported Complexes with CO.—Typically the sample (0.025 g) was placed in a glass vessel fitted with a greaseless stopcock. The vessel was evacuated and then CO introduced and the stopcock closed. Any heating was by an external resistive heating furnace and the temperature was measured using a thermocouple based digital thermometer.

Spectrum Simulation.—The calculations started with the Wilson *GF* eigenvalue problem,¹³ equation (i), where $\lambda = 4\pi^2\nu^2$ and ν is the vibrational frequency.

$$|GF - E\lambda| = 0 \quad (\text{i})$$

A standard energy-factored force field was employed, so the *G* matrix becomes diagonal with values of the inverse, reduced mass of the carbonyl groups, equation (ii), and the *F* matrix consists of the C–O stretching force constants on the diagonal,

$$G_{ii} = \frac{\mu_{\text{C}_i} + \mu_{\text{O}_i}}{\mu_{\text{C}_i}\mu_{\text{O}_i}} \quad (\text{ii})$$

with the off-diagonal terms being the interaction force constants. Symmetry was determined only by the values of these matrix elements. The eigenvalues, λ , were obtained by converting the *GF* matrix to upper Hessenberg form and solutions obtained *via* the Francis *QR* algorithm method.¹⁴ Eigenvectors were obtained from the matrix equation (iii), with (0) a zero column vector and *L* the eigenvector matrix. On the assumptions that the dipole changes in the vibrations

$$(GF - E\lambda_k)L_k = (0) \quad (\text{iii})$$

are parallel with the CO bond axis, and have the same magnitude for each ^{12}C O stretch, input of a direction cosine matrix and the normalised eigenvectors allow calculation of the intensity of the *k*th vibrational mode, I_k , by equation (iv), where k' and k'' are the indexes of the carbonyl groups. The calculated intensities and their respective frequencies were converted into a Gaussian form, so the peak areas represented relative intensity, and the peak positions the vibrational frequency. Summations of a number of chemical and/or isotopic

† *Non-S.I. units employed:* Torr = (101 325/760) N m⁻²; dyn = 10⁻⁵ N.

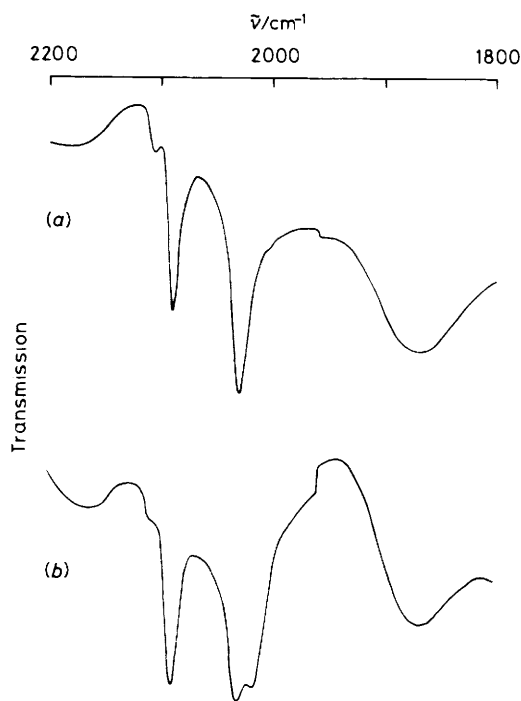


Figure 1. I.r. spectra for the reaction products of (1) and silica: (a) after 4 d at room temperature in CH_2Cl_2 ; (b) sample (a) after exposure to the i.r. beam

species could be carried out prior to plotting the resultant on a digital plotter. The experimental spectra, in absorbance, were replotted to avoid the scale change at 2000 cm^{-1} and the calculated spectra presented in a very similar form.

$$I_k = \sum_{k'k''} \cos\theta_{kk''} L_{k'k} L_{k''k} \quad (\text{iv})$$

Results

Preliminary Investigations.—The majority of cluster/oxide studies have involved deposition onto the surface, and subsequent pyrolysis of the cluster carbonyls. However, in this study, the clusters were adsorbed from solution. Because of this constant partitioning with the solvent, only relatively strongly bound species will be observed on the oxide supports and this avoids the formation of adsorbed crystallites of the cluster complexes, as has been observed for $[\text{Os}_3(\text{CO})_{12}]$.¹⁵

$[\text{Rh}_4(\text{CO})_{12}]$ (1) and silica. Solutions of (1) in dichloromethane were stirred with silica under air at room temperature. No carbonyl i.r. absorptions were observed for short reaction times, but after 4 d, an uncoloured powder was produced with i.r. bands at 2105vw , 2088w , and 2028w cm^{-1} . Allowing this species to remain as a mull in the beam of the i.r. spectrometer produced a change in which the intensity of the band at 2028 cm^{-1} decreased, a new band at 2012 cm^{-1} appeared, and the 2088 cm^{-1} absorption underwent a 5 cm^{-1} red shift (Figure 1). The reaction solution was found to contain a mixture of (1) and (2) after the reaction.

(1) and alumina. Solutions of (1) in dichloromethane were stirred with alumina at room temperature under N_2 . After 1 h, a pale mauve solid resulted, exhibiting four terminal (2083 , 2058 , 2032 , and 2002 cm^{-1}) and one weak bridging (1803 cm^{-1}) carbonyl absorptions. After 4 h in air at room temperature, the sample became bleached and its i.r. spectrum simplified to two strong bands at 2082 and 2002 cm^{-1} (Figure 2). Further exposure to air caused complete de-

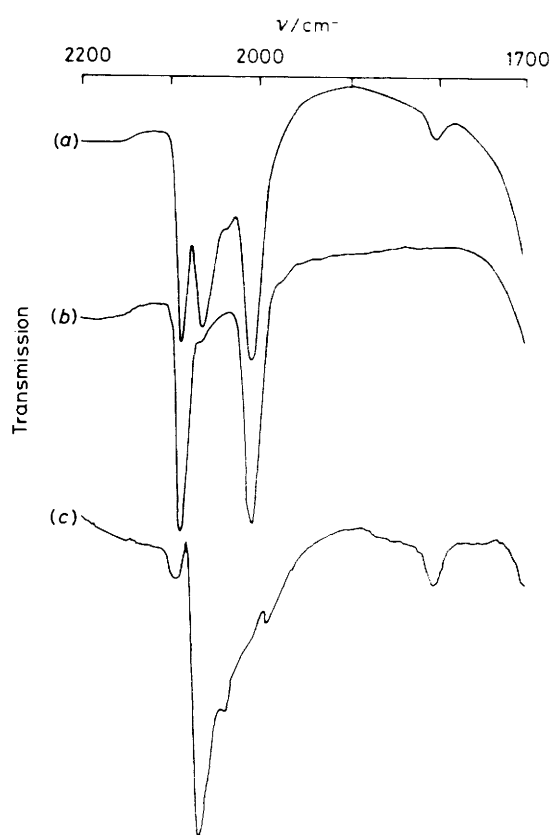


Figure 2. I.r. spectra for the reaction products of (1) and alumina: (a) after 1 h at room temperature in CH_2Cl_2 under N_2 ; (b) sample (a) after exposure to air for 1 h; (c) the difference between (a) and (b) showing the species lost on oxidation

carbonylation (after 12 h at 25°C). Allowing the impregnation reaction to continue for 4 h produced a darker mauve solid, with similar properties. Leaving a mull of this reaction product in the spectrometer beam caused the spectrum to become more complex [2096w , 2070 (sh), 2060s , 2028m , 2000s , 1860br , and 1806br cm^{-1}]. After 24 h impregnation, the oxide acquired a brown colouration, with absorptions at 2087s , 2058s , 2007vs , and 1860 — 1800br cm^{-1} and after a reaction time of 50 h, the dark powder exhibited two broad absorptions at 2000 and 1850 cm^{-1} . Over this period the supernatant also darkened and was found to have i.r. bands at 2100vw , 2078s , 2067ms , 2035w , 2013vw , and 1800w br cm^{-1} .

(1) and titania. A similar interaction of (1) with titania under N_2 was carried out and afforded a pale grey solid after 3.5 h which exhibited an i.r. spectrum with three weak absorptions at 2102w , 2085mw , and 2010mw cm^{-1} . Extending the reaction time to 6 h gave a mauve solid which showed carbonyl bands at 2102ms , 2087s , 2058m , 2041 (sh), 2007s , 1857br , and 1803w cm^{-1} . After 24 h, the solid was dark and exhibited only weak bands. Using light petrolcum (b.p. 40 — 60°C) as solvent increased the rate of the reaction, a deep mauve powder and a colourless solution being produced within 2 h.

$[\text{Rh}_6(\text{CO})_{16}]$ (2) and silica. Silica was stirred in a CH_2Cl_2 solution of (2) at room temperature but no carbonyl absorptions could be observed for the resulting solid after extended reaction times. Refluxing this reaction solution caused the oxide to darken, as did reaction mixtures in *n*-hexane (69°C), cyclohexane (80°C), or nonane (150°C). A single i.r. feature at *ca.* 2060w cm^{-1} was observed for the cyclohexane derived

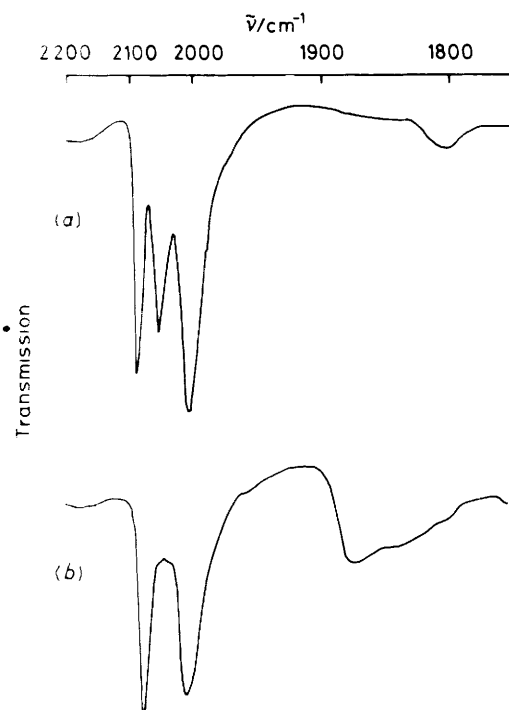


Figure 3. I.r. spectra for reaction products of (2) and alumina: (a) after 1.5 h at room temperature in CH_2Cl_2 ; (b) sample (a) after 35 min exposure to the i.r. beam

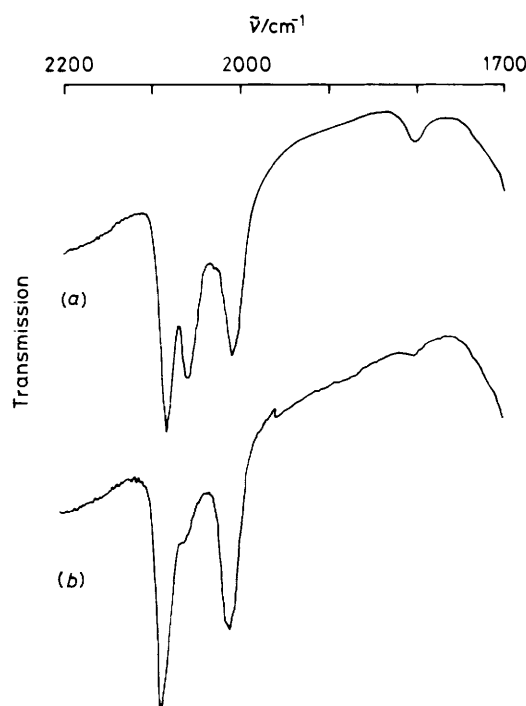


Figure 4. I.r. spectra for the reaction products of (2) and titania: (a) after 4 h at room temperature in CH_2Cl_2 ; (b) sample (a) after exposure to air for 1 h

solid after 46 h. These darkened oxides were exposed to CO at room temperature and at 240°C , but they still gave i.r. spectra showing little $\nu(\text{CO})$ intensity.

(2) and alumina. After stirring a suspension of alumina in a solution of (2) in CH_2Cl_2 under air (or N_2) for 1.5 h, a pale golden brown solid could be extracted which showed carbonyl absorptions at 2083s , 2060ms , 2004s , and 1802w br cm^{-1} . After 35 min in the spectrometer beam, the i.r. spectrum of a mull of this solid contained three bands at 2068ms , 2001ms , and $1880\text{--}1800\text{br cm}^{-1}$ (Figure 3), but this was not completely reproducible. The impregnation product was totally decarbonylated after exposure to air overnight. After interaction with CO (100 Torr) at room temperature for 40 min, the solid exhibited carbonyl bands at 2080m , 2059w , and 2002m cm^{-1} .

(2) and titania. A fawn coloured solid [$\nu(\text{CO})$ at 2080s , 2056s , 2005s , and 1802w cm^{-1}] was obtained after stirring a suspension of titania in a solution of (2) in CH_2Cl_2 under air at room temperature for 4 h. Exposure to air caused preferential loss of the bands at 2056 and 1802 cm^{-1} (Figure 4), and decarbonylation eventually became almost complete. Exposure to CO (100 Torr, room temperature, 40 min) gave a product with i.r. bands at 2082s , 2060w (sh), and 2005s cm^{-1} .

Detailed Considerations.—A common species is evident in several of these systems. Complex (1) on alumina and (2) on alumina and titania all show two strong bands of nearly equal intensity at *ca.* 2082 and *ca.* 2002 cm^{-1} . This species could also be generated by exposing the decarbonylated materials from (1) or (2) to CO. These same systems also show bands at *ca.* 2060 and 1802 cm^{-1} with intensities independent of the other two bands, and which were preferentially lost in air. Similar results have been reported¹¹ for the adsorption of CO on alumina-supported rhodium. Two bands at 2103 and 2030 cm^{-1} were assigned to the dicarbonylrhodium unit, in isolated, oxidised sites, with features at 2060 and 1860 cm^{-1}

assigned to terminal and bridging sites on rhodium crystallites. Two types of mixed carbon isotope experiments were carried out to test these conclusions.

(A) *Interaction of decarbonylated species with ^{12}CO and ^{13}CO .* Powders formed by reacting (1) or (2) with the oxide and then allowing the product to decarbonylate in air were exposed to ^{12}CO , ^{13}CO , and a mixture of the two. The observed frequencies are presented in Table 1, together with the calculated frequencies for the ^{13}CO -enriched derivatives, assuming a $\text{Rh}(\text{CO})_2$ unit of C_{2v} symmetry. A good frequency match was obtained on both alumina and titania using similar force constants, but the band intensities were investigated for further confirmation. Background subtracted spectra obtained from a sample prepared by exposing a $[\text{Rh}_4(\text{CO})_{12}]$ derived decarbonylated alumina species with ^{12}CO and a $^{12}\text{CO}/^{13}\text{CO}$ mixture are shown in Figure 5. Only absorptions due to the $\text{Rh}(\text{CO})_2$ unit were discernible, and the subtraction merely allowed for the alumina background. The typical linewidths and relative intensities of the high- and low-frequency bands were determined from the ^{12}CO spectrum. Assuming the $\text{Rh}(\text{CO})_2$ model, the intensities can be used to calculate the C–Rh–C bond angle and this, together with the measured linewidths and a value of the isotopic enrichment level (39%) were used to simulate the mixed isotope i.r. spectrum (Table 2). These simulated spectra match the experimental spectra very closely, confirming the identity of the species with i.r. absorptions at 2080 and 2002 cm^{-1} as an isolated $\text{Rh}(\text{CO})_2$ unit (C–Rh–C 94°).

(B) *Interaction of ^{13}C -enriched $[\text{Rh}_4(\text{CO})_{12}]$ with alumina.* Materials produced by interacting 40% ^{13}CO -enriched (1) with alumina and then allowing the preferential loss of the non-dicarbonyl species showed almost identical i.r. spectra to those produced in method (A). The differences evident between this spectrum and its related computer-simulated spectrum are minor and appear to be due to another species contributing to the experimental spectrum (Figure 6).

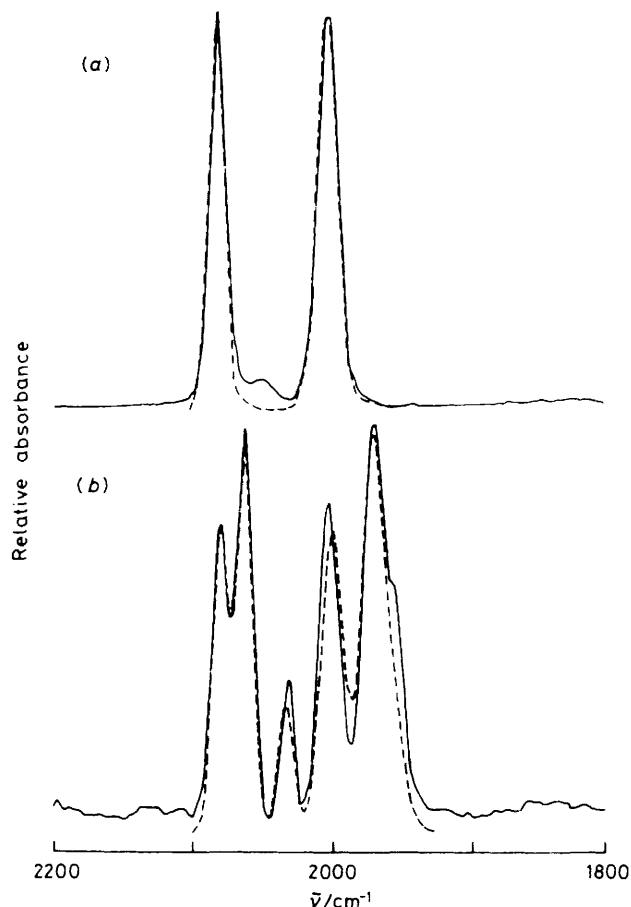


Figure 5. Experimental (—) and simulated (----) $\nu(\text{CO})$ absorption using a $\text{Rh}(\text{CO})_2$ model, for the decarbonylated $\text{Rh}/\text{Al}_2\text{O}_3$ powder after exposure (a) to ^{12}CO and (b) to a $^{12}\text{CO}/^{13}\text{CO}$ mixture

The i.r. spectrum of the other species initially present in the mauve material formed by interacting (1) and alumina was obtained by taking the difference between the spectra (a) and (b) in Figure 2. Two of the bands due to this species, giving the spectrum in Figure 2(c), could either be due to terminal and bridge sites of CO on metal crystallites, reported at ca. 2 060 and 1 860 cm^{-1} respectively¹¹ or at ca. 2 035–2 025 and 1 850–1 825 cm^{-1} by Basset and co-workers,^{6,7} or they could be assigned to $[\text{Rh}_6(\text{CO})_{16}]$, reported as showing $\nu(\text{CO})$ bands at 2 058 and 1 830 cm^{-1} on alumina pretreated at 200 °C.^{6,7}

A spectrum very similar *in profile* to the original spectrum obtained when (1) was reacted with alumina was obtained when a previously decarbonylated $\text{Rh}/\text{Al}_2\text{O}_3$ powder was exposed to ^{13}CO (200 Torr) at 50 °C for 5 h (Figure 7). The expected isotopic shift is seen for all bands, the only distinct difference being an extra weak band at 2 010 cm^{-1} which can be assigned to the symmetric stretch of a $\text{Rh}(^{12}\text{CO})(^{13}\text{CO})$ species. The similarity of the profiles indicates that CO loss is reversible. Similar exposure to a 35% $^{12}\text{CO}/^{13}\text{CO}$ mixture afforded the spectrum in Figure 7(b), showing two distinct i.r. absorptions in the bridging $\nu(\text{CO})$ region at 1 802 and 1 762 cm^{-1} , the intensities of which reflect the isotopic proportions. These bands correspond to those observed in the all- ^{12}C and all- ^{13}C samples respectively. This observation suggests the presence of a bridging monocarbonyl species since strong bands of intermediate frequency would be anticipated from (2), with four bridging groups. The i.r.

Table 1. Observed and calculated frequencies for decarbonylated supported rhodium exposed to CO^a

Experiment	Observed frequency (cm^{-1})	Calculated frequency (cm^{-1}) for $\text{Rh}(\text{CO})_2$ unit
(2) $^{b}/\text{Al}_2\text{O}_3 + ^{12}\text{CO}$ (40 Torr, 300 K, 15 min)	2 080m 2 059w	2 080.0
(2) $^{b}/\text{Al}_2\text{O}_3 + ^{13}\text{CO}$ (40 Torr, 300 K, 15 min)	2 002m 2 061w 2 031m	2 002.0 2 033.8
(2) $^{b}/\text{Al}_2\text{O}_3 + ^{12}\text{CO}/^{13}\text{CO}$ (80 Torr, 300 K, 15 min)	1 956m 2 080s 2 062m 2 002s 1 973m	1 957.5 2 080.0, $\text{M}(^{12}\text{CO})_2$ 2 063.1, $\text{M}(^{12}\text{CO})(^{13}\text{CO})$ 2 002.0, $\text{M}(^{12}\text{CO})_2$ 1 973.6, $\text{M}(^{12}\text{CO})(^{13}\text{CO})$
(2) $\text{TiO}_2 + ^{12}\text{CO}$ (100 Torr, 300 K, 40 min)	2 082s 2 060w 2 005s	2 082.0 2 005.0
(2) $\text{TiO}_2 + ^{13}\text{CO}$ (100 Torr, 300 K, 40 min)	2 060w 2 033s 2 010w 1 959s	2 035.7 1 960.4
(2) $\text{TiO}_2 + ^{12}\text{CO}/^{13}\text{CO}$ (100 Torr, 300 K, 40 min)	2 063m 2 031m 1 977m 1 960m	2 065.1, $\text{M}(^{12}\text{CO})(^{13}\text{CO})$ 2 035.7, $\text{M}(^{13}\text{CO})_2$ 1 976.5, $\text{M}(^{12}\text{CO})(^{13}\text{CO})$ 1 960.4, $\text{M}(^{13}\text{CO})_2$

^a Force constants: $K = 16.84$, $k_1 = 0.64$ $\text{mdyn } \text{Å}^{-1}$ on alumina; $K = 16.88$, $k_1 = 0.66$ $\text{mdyn } \text{Å}^{-1}$ on titania. ^b Identical results using a decarbonylated $[\text{Rh}_6(\text{CO})_{12}]$ derived material.

Table 2. Observed and calculated parameters for the $\text{Rh}(\text{CO})_2$ species obtained on exposure of a decarbonylated $\text{Rh}/\text{Al}_2\text{O}_3$ sample to CO (natural abundance)

Frequency ^a (cm^{-1})	Relative intensity ^b	Linewidth (cm^{-1})
2 081 (2 081)	1.0	13
2 002 (2 002)	1.16	18

^a Calculated values in parentheses: $K = 16.84$, $k_1 = 0.65$ $\text{mdyn } \text{Å}^{-1}$.
^b C–Rh–C = 94.2°.

spectrum of a partially enriched sample of (2) did show intermediate intensity, but the strongest bands were those at the extremes of the isotopic shift. This is in accord with the natural abundance spectrum observed by Cariati *et al.*,¹⁶ showing the interaction between the μ_3 -CO groups in (2) to be small. So, allowing for the complications due to the surface environment, this species giving rise to the band at 1 802 cm^{-1} could be (2). Indeed, Watters *et al.*⁴ extracted (2) from alumina into chloroform solution under a CO atmosphere.

A similar experiment, but in the absence of CO, was carried out on titania, which also shows this species (Figure 4). A purple sample derived from interacting this oxide with a solution of (1) in light petroleum (b.p. 40–60 °C) was washed with boiling tetrahydrofuran. The support showed three bands obtained by interacting (1) with titania over a short reaction time, and the dissolved material gave rise to an i.r. spectrum (recorded in cyclohexane) which indicated that (2) was the major component with no residual compound (1). It therefore appears that (1) is partially converted to (2) on both alumina and titania.

This three-band pattern (2 101, 2 083, and 2 010 cm^{-1} ; relative intensities 0.25 : 0.85 : 1.0) formed from the reaction between (1) and titania, is different from the two-band spectrum analysed above, and is similar to that of $\{[\text{Rh}(\text{CO})_2\text{-Cl}]_2\}$ (3) (2 105, 2 089, and 2 034 cm^{-1}). Spectra of samples

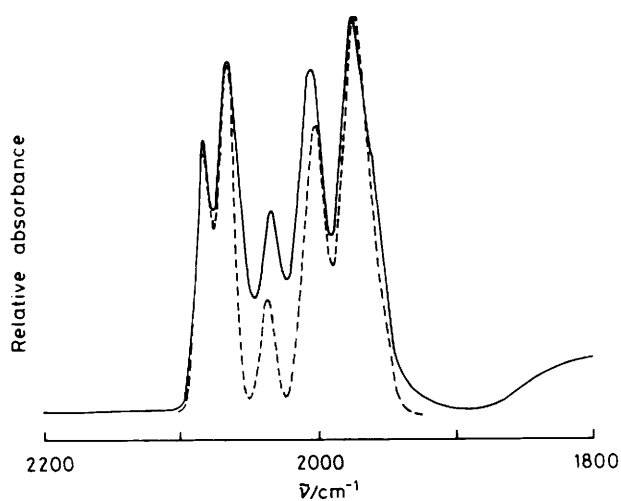


Figure 6. Experimental (—) i.r. spectrum obtained by the reaction of 39% ^{13}CO -enriched (1) with alumina (after background subtraction) and the computed spectrum (---) using a $\text{M}(\text{CO})_2$ model

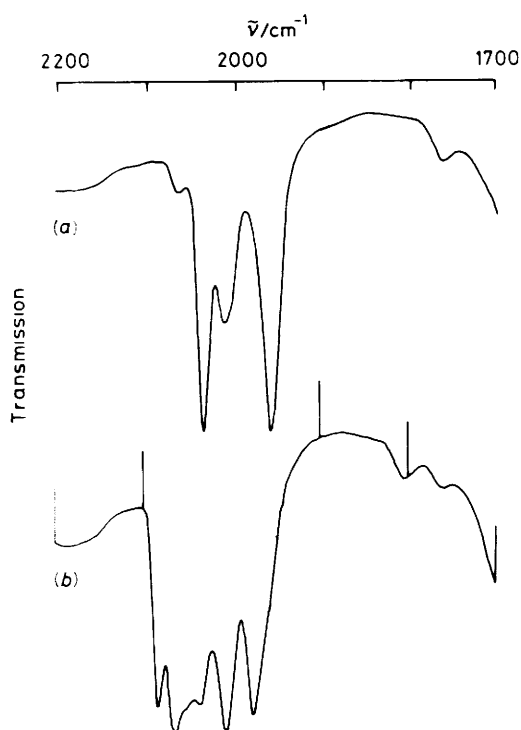


Figure 7. Initial i.r. spectra obtained on exposing a decarbonylated $\text{Rh}/\text{Al}_2\text{O}_3$ powder (a) to ^{13}CO and (b) to a $^{12}\text{CO}/^{13}\text{CO}$ mixture

prepared with natural abundance and 40% ^{13}CO -enriched (1) are shown in Figure 8.

The initial model chosen to simulate these spectra was that of (3), for which a force field has been established by C^{18}O exchange studies¹⁷ ($K = 17.254$, $k_{\text{gem}} = 0.541$, $k_{\text{trans}} = 0.057$, and $k_{\text{cis}} = 0.078$ $\text{mdyn } \text{Å}^{-1}$). A frequency match for the supported species with natural abundance CO could be obtained by altering two of these values, K and k_{gem} to 17.0 and 0.7 $\text{mdyn } \text{Å}^{-1}$, respectively. Whilst this is not a unique solution, this forms a good estimate of these values for reasonable magnitudes of k_{trans} and k_{cis} . The relative intensities

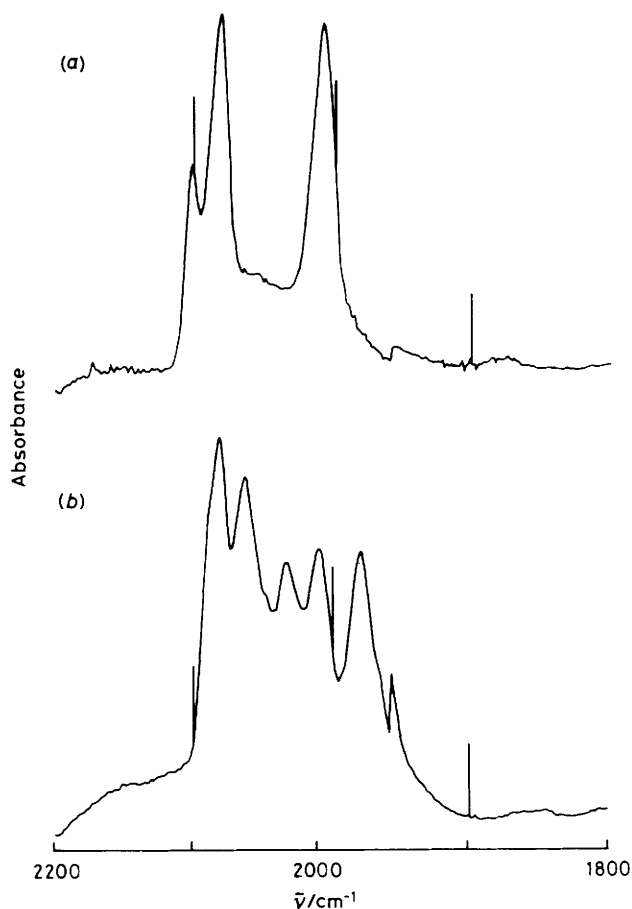
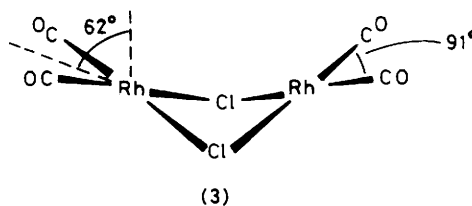


Figure 8. I.r. spectra for the reaction products of (1) and titania: (a) natural abundance CO; (b) 40% ^{13}CO -enriched CO



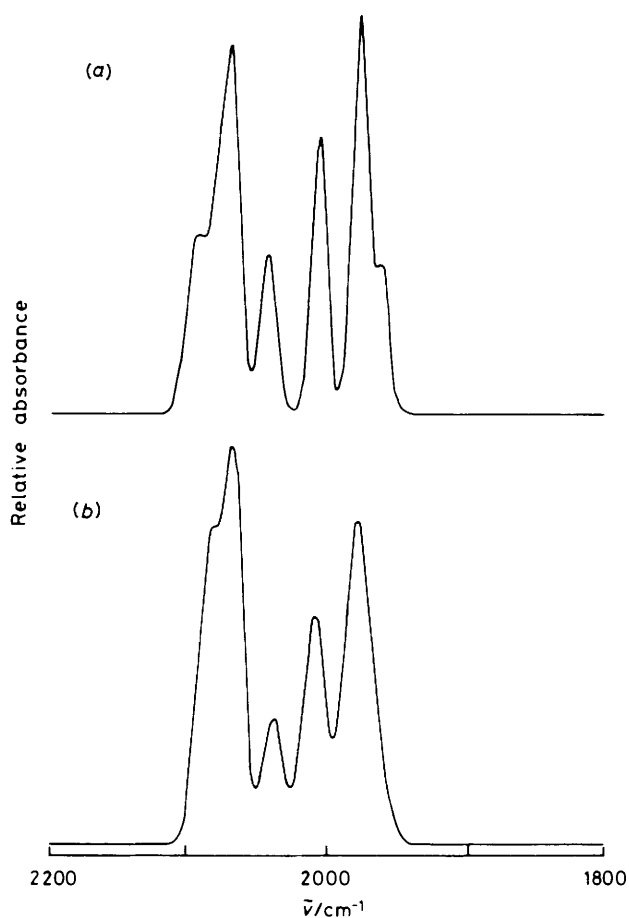
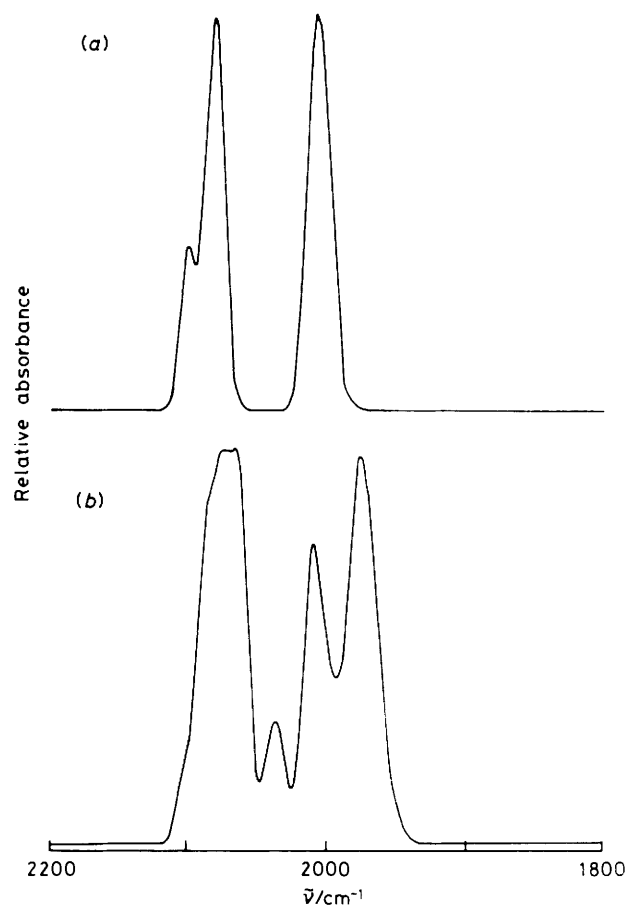
could be matched by reducing the *geminal* C-Rh-C angle to 87° , whilst keeping a dihedral angle of 62° between the $\text{Rh}(\text{CO})_2$ plane and the direction of the C_2 axis. The mixed isotope simulation is presented in Figure 9(a).

If the high-frequency band is independent of the other two bands, then much of the pattern should be reproducible using the $\text{Rh}(\text{CO})_2$ model. The calculated mixed isotope spectrum is presented in Figure 9(b). This is a closer match of the experimental spectrum [Figure 8(b)] than that of the dimer model. However, the intensity match is poor since the calculated spectrum contains a clear shoulder at 2093 cm^{-1} and the experimental spectrum contains intensity due to another species in the region $2000\text{--}2050 \text{ cm}^{-1}$. Freely floating the force field for the $[\{\text{Rh}(\text{CO})_2\text{Cl}\}_2]$ model did not improve on the calculated spectrum in Figure 9(a). It is therefore probable that the experimental spectrum is due to an isolated $\text{Rh}(\text{CO})_2$ unit and a second carbonyl species. This is clearly not a monocarbonyl, since the enrichment level would lead to the band being at 2102 cm^{-1} at 60% of its original intensity. Very

Table 3. Combinations of C-Rh-C bond angles allowed to simulate the ^{12}CO spectrum of the species formed from (1) and TiO_2 using a two-species model *

$\text{Rh}(\text{CO})_2$			$\text{Rh}(\text{CO})_3$			$\text{Rh}(\text{CO})_4$		
Angle ($^\circ$)	I_{a_1}	I_{b_1}	Angle ($^\circ$)	I_{a_1}	I_e	Angle ($^\circ$)	I_{a_1}	I_e
90	0.85	0.85	64	0.25	0.15	51.5	0.25	0.15
85	0.85	0.714	78.5	0.25	0.286	62	0.25	0.286
80	0.85	0.598	85.7	0.25	0.402	67.5	0.25	0.402
75	0.85	0.5	90	0.25	0.5	70.5	0.25	0.5

* Total intensities: $I_{a_1}[\text{M}(\text{CO})_n; n = 3 \text{ or } 4] = 0.25$, $I_{a_1}[\text{M}(\text{CO})_2] = 0.85$; $I_{b_1} + I_e = 1.0$.

**Figure 9.** Computed i.r. spectra for the reaction products of ^{13}CO -enriched (1) and titania using (a) a $[\text{M}(\text{CO})_2]_2$ model and (b) a $\text{M}(\text{CO})_2$ model**Figure 10.** Computed i.r. spectra for the reaction products of (1) and titania using a $\text{M}(\text{CO})_2/\text{M}(\text{CO})_3$ model: (a) ^{12}CO ; (b) ^{13}CO -enriched

little intensity is observed at that frequency, so species with more carbonyls per rhodium atom are suggested. Tetra-, tri-, and di-carbonyls would be expected to exhibit 13, 21.5, and 36% respectively of the ^{12}CO band intensity at that point; the first two therefore seem more probable.

For a $\text{M}(\text{CO})_n$ species ($n > 2$) to exhibit a single i.r.-active mode, high symmetry is required. For $n = 4$, T_d symmetry will allow this; $\text{Rh}(\text{CO})_4^-$ exhibits an i.r. band at *ca.* 1900 cm^{-1} ¹⁸ and the hypothetical $\text{Rh}(\text{CO})_4^+$ is unlikely. In addition, the effective lowering of symmetry caused by partial ^{13}CO substitution would give i.r.-active bands at a higher frequency than the t_2 mode, none of which was observed. A D_{4h} geometry would also show this effect. Therefore the band at 2102 cm^{-1} must be associated with another band obscured by one of the $\text{M}(\text{CO})_2$ absorptions, the lower frequency one being

more likely. Spectra assuming the experimental spectrum to be (i) a $\text{Rh}(\text{CO})_2\text{-Rh}(\text{CO})_3$ mixture and (ii) a $\text{Rh}(\text{CO})_2\text{-Rh}(\text{CO})_4$ mixture were calculated. If the low-frequency band is assumed to be the b_1 mode for the dicarbonyl plus the e mode of either a C_{3v} $\text{Rh}(\text{CO})_3$ or C_{4v} $\text{Rh}(\text{CO})_4$ unit, then the observed relative intensities give an allowed set of C-Rh-C angles some of which are listed in Table 3. Expected bond angles are *ca.* 90° , *ca.* 90° , and *ca.* 76° for the $\text{M}(\text{CO})_2$, $\text{M}(\text{CO})_3$, and $\text{M}(\text{CO})_4$ moieties respectively. Of the combinations listed for (i), the most viable pairing is $\text{M}(\text{CO})_2$, 85° , and $\text{M}(\text{CO})_3$, 78.5° ; for (ii) the combination of 80 and 67.5° for di- and tetra-carbonyl units is most probable. Spectra calculated for both these models, using the linewidths observed in the ^{12}CO spectra are given in Figures 10 and 11 for (i) and (ii) respectively. A ratio of $k_{\text{trans}} : k_{\text{cis}}$ of 1.63 was used for (ii), based on

not require there to be a cluster derived grouping. Rather it parallels the synthesis of (2).¹² Our evidence, albeit less clearly in this case, is also opposed to the suggestion of a dimeric $[\{\text{Rh}(\text{CO})_2\text{Cl}\}_2]$ type structure on silica.²¹ The isolation of these fragmented rhodium carbonyl centres is, however, in accord with a variety of data obtained on conventionally prepared alumina-supported rhodium.¹¹ The frequencies of the two $\nu(\text{CO})$ bands of the $\text{Rh}(\text{CO})_2$ sites vary significantly between research groups, e.g. from 2105 and 2040 cm^{-1} (ref. 6) to 2080 and 1997 cm^{-1} (ref. 10). It is clear that the type of alumina used and the water content both affect these frequencies. Somewhat higher frequencies have been reported on the same alumina as used in our studies.²² However, sampling then was in pressed discs and we have noted ca. 8 cm^{-1} shifts to high frequency for pressed oxide discs compared with Nujol mulls. In all cases, it is probable that the rhodium is in the +1 oxidation state, and the varying water content affects the electron density available to the carbonyl groups transmitted through the rhodium and the surface oxygen atoms to which it is bound.

It has been shown that oxidative fragmentation can be spontaneous on alumina, while oxygen is required on silica.^{6,7} It seems also from the partitioning nature of our adsorption experiments that even in the presence of oxygen, (1) and especially (2) form supported rhodium sites very slowly on silica. Evidently a strong surface cluster interaction is required initially and this is not possible for silica. This does occur on alumina and titania, probably involving Lewis acid sites. We note also the photochemical changes occurring in the i.r. beam, particularly the probable aggregation on alumina.

Acknowledgements

We wish to thank the S.E.R.C. for a research studentship (to G. S. McN.), Dr. J. S. Ogden for helpful discussions, and Degussa Ltd. for chemicals.

References

- 1 J. Robertson and G. Webb, *Proc. R. Soc. London, Ser. A*, 1974, **341**, 383.
- 2 G. C. Smith, T. P. Chojnacki, S. R. Dasgupta, K. Iwatate, and K. L. Watters, *Inorg. Chem.*, 1975, **14**, 1419.

- 3 S. L. T. Andersson, K. L. Watters, and R. F. Howe, *J. Catal.*, 1981, **69**, 212.
- 4 K. L. Watters, R. F. Howe, T. P. Chojnacki, C.-M. Fu, R. L. Schneider, and N.-B. Wong, *J. Catal.*, 1980, **66**, 424.
- 5 R. Ugo, R. Psaro, G. M. Zanderighi, J. M. Basset, A. Theolier, and A. K. Smith, *Fundam. Res. Homogeneous Catal.*, 1979, **3**, 579.
- 6 A. K. Smith, F. Hugues, A. Theolier, J. M. Basset, R. Ugo, G. M. Zanderighi, J. L. Bilhou, V. Bilhou-Bougnol, and W. F. Graydon, *Inorg. Chem.*, 1979, **18**, 3104.
- 7 A. Theolier, A. K. Smith, M. Leconte, J. M. Basset, G. M. Zanderighi, R. Psaro, and R. Ugo, *J. Organomet. Chem.*, 1980, **191**, 415.
- 8 M. Ichikawa, *Bull. Chem. Soc. Jpn.*, 1978, **51**, 2273.
- 9 D. A. Hucul and A. Brenner, *J. Phys. Chem.*, 1981, **85**, 496.
- 10 P. Michelin Lausarot, G. A. Vaglio, and M. Valle, *J. Organomet. Chem.*, 1981, **204**, 249.
- 11 A. C. Yang and C. W. Garland, *J. Phys. Chem.*, 1957, **61**, 1504; J. T. Yates, jun., T. M. Duncan, and R. W. Vaughan, *J. Chem. Phys.*, 1979, **71**, 3908; R. R. Cavanagh and J. T. Yates, jun., *ibid.*, 1981, **74**, 4150; C. A. Rice, S. D. Worley, C. W. Curtis, J. A. Guin, and A. R. Tarrer, *ibid.*, 1981, **74**, 6487; T. M. Duncan, J. T. Yates, jun., and R. W. Vaughan, *ibid.*, 1979, **71**, 3129; 1980, **73**, 975.
- 12 P. Chini and S. Martinengo, *Inorg. Chim. Acta*, 1969, **3**, 315.
- 13 E. B. Wilson, jun., J. C. Decius, and P. C. Cross, 'Molecular Vibrations,' McGraw-Hill, New York, 1955.
- 14 J. H. Wilkinson and C. Reinsch, 'Handbook for Automatic Computation Linear Algebra,' Springer-Verlag, Berlin, 1971, vol. 2.
- 15 G. Collier, D. J. Hunt, S. D. Jackson, R. B. Moyes, I. A. Pickering, P. B. Wells, A. F. Simpson, and R. Whyman, *J. Catal.*, 1983, **80**, 154.
- 16 F. Cariati, V. Valenti, and P. Barona, *Gazz. Chim. Ital.*, 1969, **99**, 1327.
- 17 B. F. G. Johnson, J. Lewis, P. W. Robinson, and J. R. Miller, *J. Chem. Soc. A*, 1969, 2693.
- 18 P. Chini and S. Martinengo, *Inorg. Chim. Acta*, 1969, **3**, 21.
- 19 J. R. Durig, R. B. King, L. W. Houk, and A. L. Marston, *J. Organomet. Chem.*, 1969, **16**, 425.
- 20 N. A. Bailey, E. Coates, G. B. Robertson, F. Bonati, and R. Ugo, *Chem. Commun.*, 1967, 1041.
- 21 R. Whyman, in 'Transition Metal Clusters,' ed. B. F. G. Johnson, Wiley, New York, 1980.
- 22 S. D. Worley, C. A. Rice, G. A. Mattson, C. W. Curtis, J. A. Guin, and A. R. Tarrer, *J. Chem. Phys.*, 1982, **76**, 20.

Received 10th June 1983; Paper 3/968